



Study of Υ production and cold nuclear matter effects in $p\text{Pb}$ collisions at $\sqrt{s_{NN}} = 5 \text{ TeV}$

The LHCb collaboration[†]

Abstract

Production of Υ mesons in proton-lead collisions at a nucleon-nucleon centre-of-mass energy $\sqrt{s_{NN}} = 5 \text{ TeV}$ is studied with the LHCb detector. The analysis is based on a data sample corresponding to an integrated luminosity of 1.6 nb^{-1} . The Υ mesons of transverse momenta up to $15 \text{ GeV}/c$ are reconstructed in the dimuon decay mode. The rapidity coverage in the centre-of-mass system is $1.5 < y < 4.0$ (forward region) and $-5.0 < y < -2.5$ (backward region). The forward-backward production ratio and the nuclear modification factor for $\Upsilon(1S)$ mesons are determined. The data are compatible with the predictions for a suppression of $\Upsilon(1S)$ production with respect to proton-proton collisions in the forward region, and an enhancement in the backward region. The suppression is found to be smaller than in the case of prompt J/ψ mesons.

published in JHEP

© CERN on behalf of the LHCb collaboration, license CC-BY-3.0.

[†]Authors are listed on the following pages.

LHCb collaboration

R. Aaij⁴¹, B. Adeva³⁷, M. Adinolfi⁴⁶, A. Affolder⁵², Z. Ajaltouni⁵, J. Albrecht⁹, F. Alessio³⁸, M. Alexander⁵¹, S. Ali⁴¹, G. Alkhazov³⁰, P. Alvarez Cartelle³⁷, A.A. Alves Jr^{25,38}, S. Amato², S. Amerio²², Y. Amhis⁷, L. An³, L. Anderlini^{17,g}, J. Anderson⁴⁰, R. Andreassen⁵⁷, M. Andreotti^{16,f}, J.E. Andrews⁵⁸, R.B. Appleby⁵⁴, O. Aquines Gutierrez¹⁰, F. Archilli³⁸, A. Artamonov³⁵, M. Artuso⁵⁹, E. Aslanides⁶, G. Auriemma^{25,n}, M. Baalouch⁵, S. Bachmann¹¹, J.J. Back⁴⁸, A. Badalov³⁶, V. Balagura³¹, W. Baldini¹⁶, R.J. Barlow⁵⁴, C. Barschel³⁸, S. Barsuk⁷, W. Barter⁴⁷, V. Batozkaya²⁸, A. Bay³⁹, L. Beaucourt⁴, J. Beddow⁵¹, F. Bedeschi²³, I. Bediaga¹, S. Belogurov³¹, K. Belous³⁵, I. Belyaev³¹, E. Ben-Haim⁸, G. Bencivenni¹⁸, S. Benson³⁸, J. Benton⁴⁶, A. Berezhnoy³², R. Bernet⁴⁰, M.-O. Bettler⁴⁷, M. van Beuzekom⁴¹, A. Bien¹¹, S. Bifani⁴⁵, T. Bird⁵⁴, A. Bizzeti^{17,i}, P.M. Bjørnstad⁵⁴, T. Blake⁴⁸, F. Blanc³⁹, J. Blouw¹⁰, S. Blusk⁵⁹, V. Bocci²⁵, A. Bondar³⁴, N. Bondar^{30,38}, W. Bonivento^{15,38}, S. Borghi⁵⁴, A. Borgia⁵⁹, M. Borsato⁷, T.J.V. Bowcock⁵², E. Bowen⁴⁰, C. Bozzi¹⁶, T. Brambach⁹, J. van den Brand⁴², J. Bressieux³⁹, D. Brett⁵⁴, M. Britsch¹⁰, T. Britton⁵⁹, J. Brodzicka⁵⁴, N.H. Brook⁴⁶, H. Brown⁵², A. Bursche⁴⁰, G. Busetto^{22,q}, J. Buytaert³⁸, S. Cadeddu¹⁵, R. Calabrese^{16,f}, M. Calvi^{20,k}, M. Calvo Gomez^{36,o}, A. Camboni³⁶, P. Campana^{18,38}, D. Campora Perez³⁸, A. Carbone^{14,d}, G. Carboni^{24,l}, R. Cardinale^{19,38,j}, A. Cardini¹⁵, H. Carranza-Mejia⁵⁰, L. Carson⁵⁰, K. Carvalho Akiba², G. Casse⁵², L. Cassina²⁰, L. Castillo Garcia³⁸, M. Cattaneo³⁸, Ch. Cauet⁹, R. Cenci⁵⁸, M. Charles⁸, Ph. Charpentier³⁸, S. Chen⁵⁴, S.-F. Cheung⁵⁵, N. Chiapolini⁴⁰, M. Chrzaszcz^{40,26}, K. Ciba³⁸, X. Cid Vidal³⁸, G. Ciezarek⁵³, P.E.L. Clarke⁵⁰, M. Clemencic³⁸, H.V. Cliff⁴⁷, J. Closier³⁸, V. Coco³⁸, J. Cogan⁶, E. Cogneras⁵, P. Collins³⁸, A. Comerma-Montells¹¹, A. Contu^{15,38}, A. Cook⁴⁶, M. Coombes⁴⁶, S. Coquereau⁸, G. Corti³⁸, M. Corvo^{16,f}, I. Counts⁵⁶, B. Couturier³⁸, G.A. Cowan⁵⁰, D.C. Craik⁴⁸, M. Cruz Torres⁶⁰, S. Cunliffe⁵³, R. Currie⁵⁰, C. D'Ambrosio³⁸, J. Dalsen⁴⁶, P. David⁸, P.N.Y. David⁴¹, A. Davis⁵⁷, K. De Bruyn⁴¹, S. De Capua⁵⁴, M. De Cian¹¹, J.M. De Miranda¹, L. De Paula², W. De Silva⁵⁷, P. De Simone¹⁸, D. Decamp⁴, M. Deckenhoff⁹, L. Del Buono⁸, N. Déleage⁴, D. Derkach⁵⁵, O. Deschamps⁵, F. Dettori⁴², A. Di Canto³⁸, H. Dijkstra³⁸, S. Donleavy⁵², F. Dordei¹¹, M. Dorigo³⁹, A. Dosil Suárez³⁷, D. Dossett⁴⁸, A. Dovbnya⁴³, G. Dujany⁵⁴, F. Dupertuis³⁹, P. Durante³⁸, R. Dzhelyadin³⁵, A. Dziurda²⁶, A. Dzyuba³⁰, S. Easo^{49,38}, U. Egede⁵³, V. Egorychev³¹, S. Eidelman³⁴, S. Eisenhardt⁵⁰, U. Eitschberger⁹, R. Ekelhof⁹, L. Eklund^{51,38}, I. El Rifai⁵, Ch. Elsasser⁴⁰, S. Ely⁵⁹, S. Esen¹¹, T. Evans⁵⁵, A. Falabella^{16,f}, C. Färber¹¹, C. Farinelli⁴¹, N. Farley⁴⁵, S. Farry⁵², D. Ferguson⁵⁰, V. Fernandez Albor³⁷, F. Ferreira Rodrigues¹, M. Ferro-Luzzi³⁸, S. Filippov³³, M. Fiore^{16,f}, M. Fiorini^{16,f}, M. Firlej²⁷, C. Fitzpatrick³⁸, T. Fiutowski²⁷, M. Fontana¹⁰, F. Fontanelli^{19,j}, R. Forty³⁸, O. Francisco², M. Frank³⁸, C. Frei³⁸, M. Frosini^{17,38,g}, J. Fu^{21,38}, E. Furfaro^{24,l}, A. Gallas Torreira³⁷, D. Galli^{14,d}, S. Gallorini²², S. Gambetta^{19,j}, M. Gandelman², P. Gandini⁵⁹, Y. Gao³, J. Garofoli⁵⁹, J. Garra Tico⁴⁷, L. Garrido³⁶, C. Gaspar³⁸, R. Gauld⁵⁵, L. Gavardi⁹, E. Gersabeck¹¹, M. Gersabeck⁵⁴, T. Gershon⁴⁸, Ph. Ghez⁴, A. Gianelle²², S. Giani³⁹, V. Gibson⁴⁷, L. Giubega²⁹, V.V. Gligorov³⁸, C. Göbel⁶⁰, D. Golubkov³¹, A. Golutvin^{53,31,38}, A. Gomes^{1,a}, H. Gordon³⁸, C. Gotti²⁰, M. Grabalosa Gándara⁵, R. Graciani Diaz³⁶, L.A. Granado Cardoso³⁸, E. Graugés³⁶, G. Graziani¹⁷, A. Grecu²⁹, E. Greening⁵⁵, S. Gregson⁴⁷, P. Griffith⁴⁵, L. Grillo¹¹, O. Grünberg⁶², B. Gui⁵⁹, E. Gushchin³³, Yu. Guz^{35,38}, T. Gys³⁸, C. Hadjivasiliou⁵⁹, G. Haefeli³⁹, C. Haen³⁸, S.C. Haines⁴⁷, S. Hall⁵³, B. Hamilton⁵⁸, T. Hampson⁴⁶, X. Han¹¹, S. Hansmann-Menzemer¹¹, N. Harnew⁵⁵, S.T. Harnew⁴⁶, J. Harrison⁵⁴, T. Hartmann⁶², J. He³⁸, T. Head³⁸, V. Heijne⁴¹, K. Hennessy⁵², P. Henrard⁵, L. Henry⁸,

J.A. Hernando Morata³⁷, E. van Herwijnen³⁸, M. Heß⁶², A. Hicheur¹, D. Hill⁵⁵, M. Hoballah⁵,
 C. Hombach⁵⁴, W. Hulsbergen⁴¹, P. Hunt⁵⁵, N. Hussain⁵⁵, D. Hutchcroft⁵², D. Hynds⁵¹,
 M. Idzik²⁷, P. Ilten⁵⁶, R. Jacobsson³⁸, A. Jaeger¹¹, J. Jalocha⁵⁵, E. Jans⁴¹, P. Jatón³⁹,
 A. Jawahery⁵⁸, M. Jezabek²⁶, F. Jing³, M. John⁵⁵, D. Johnson⁵⁵, C.R. Jones⁴⁷, C. Joram³⁸,
 B. Jost³⁸, N. Jurik⁵⁹, M. Kaballo⁹, S. Kandybei⁴³, W. Kanso⁶, M. Karacson³⁸, T.M. Karbach³⁸,
 M. Kelsey⁵⁹, I.R. Kenyon⁴⁵, T. Ketel⁴², B. Khanji²⁰, C. Khurewathanakul³⁹, S. Klaver⁵⁴,
 O. Kochebina⁷, M. Kolpin¹¹, I. Komarov³⁹, R.F. Koopman⁴², P. Koppenburg^{41,38}, M. Korolev³²,
 A. Kozlinskiy⁴¹, L. Kravchuk³³, K. Kreplin¹¹, M. Kreps⁴⁸, G. Krocker¹¹, P. Krokovny³⁴,
 F. Kruse⁹, M. Kucharczyk^{20,26,38,k}, V. Kudryavtsev³⁴, K. Kurek²⁸, T. Kvaratskheliya³¹,
 V.N. La Thi³⁹, D. Lacarrere³⁸, G. Lafferty⁵⁴, A. Lai¹⁵, D. Lambert⁵⁰, R.W. Lambert⁴²,
 E. Lanciotti³⁸, G. Lanfranchi¹⁸, C. Langenbruch³⁸, B. Langhans³⁸, T. Latham⁴⁸, C. Lazzeroni⁴⁵,
 R. Le Gac⁶, J. van Leerdam⁴¹, J.-P. Lees⁴, R. Lefèvre⁵, A. Leflat³², J. Lefrançois⁷, S. Leo²³,
 O. Leroy⁶, T. Lesiak²⁶, B. Leverington¹¹, Y. Li³, M. Liles⁵², R. Lindner³⁸, C. Linn³⁸,
 F. Lionetto⁴⁰, B. Liu¹⁵, G. Liu³⁸, S. Lohn³⁸, I. Longstaff⁵¹, J.H. Lopes², N. Lopez-March³⁹,
 P. Lowdon⁴⁰, H. Lu³, D. Lucchesi^{22,q}, H. Luo⁵⁰, A. Lupato²², E. Luppi^{16,f}, O. Lupton⁵⁵,
 F. Machefert⁷, I.V. Machikhiliyan³¹, F. Maciuc²⁹, O. Maev³⁰, S. Malde⁵⁵, G. Manca^{15,e},
 G. Mancinelli⁶, M. Manzali^{16,f}, J. Maratas⁵, J.F. Marchand⁴, U. Marconi¹⁴, C. Marin Benito³⁶,
 P. Marino^{23,s}, R. Märki³⁹, J. Marks¹¹, G. Martellotti²⁵, A. Martens⁸, A. Martín Sánchez⁷,
 M. Martinelli⁴¹, D. Martinez Santos⁴², F. Martinez Vidal⁶⁴, D. Martins Tostes², A. Massafferri¹,
 R. Matev³⁸, Z. Mathe³⁸, C. Matteuzzi²⁰, A. Mazurov^{16,f}, M. McCann⁵³, J. McCarthy⁴⁵,
 A. McNab⁵⁴, R. McNulty¹², B. McSkelly⁵², B. Meadows^{57,55}, F. Meier⁹, M. Meissner¹¹,
 M. Merk⁴¹, D.A. Milanese⁸, M.-N. Minard⁴, N. Moggi¹⁴, J. Molina Rodriguez⁶⁰, S. Monteil⁵,
 D. Moran⁵⁴, M. Morandin²², P. Morawski²⁶, A. Mordà⁶, M.J. Morello^{23,s}, J. Moron²⁷,
 A.-B. Morris⁵⁰, R. Mountain⁵⁹, F. Muheim⁵⁰, K. Müller⁴⁰, R. Muresan²⁹, M. Mussini¹⁴,
 B. Muster³⁹, P. Naik⁴⁶, T. Nakada³⁹, R. Nandakumar⁴⁹, I. Nasteva², M. Needham⁵⁰, N. Neri²¹,
 S. Neubert³⁸, N. Neufeld³⁸, M. Neuner¹¹, A.D. Nguyen³⁹, T.D. Nguyen³⁹, C. Nguyen-Mau^{39,p},
 M. Nicol⁷, V. Niess⁵, R. Niet⁹, N. Nikitin³², T. Nikodem¹¹, A. Novoselov³⁵,
 A. Oblakowska-Mucha²⁷, V. Obraztsov³⁵, S. Oggero⁴¹, S. Ogilvy⁵¹, O. Okhrimenko⁴⁴,
 R. Oldeman^{15,e}, G. Onderwater⁶⁵, M. Orlandea²⁹, J.M. Otalora Goicochea², P. Owen⁵³,
 A. Oyanguren⁶⁴, B.K. Pal⁵⁹, A. Palano^{13,c}, F. Palombo^{21,t}, M. Palutan¹⁸, J. Panman³⁸,
 A. Papanestis^{49,38}, M. Pappagallo⁵¹, C. Parkes⁵⁴, C.J. Parkinson⁹, G. Passaleva¹⁷, G.D. Patel⁵²,
 M. Patel⁵³, C. Patrignani^{19,j}, A. Pazos Alvarez³⁷, A. Pearce⁵⁴, A. Pellegrino⁴¹,
 M. Pepe Altarelli³⁸, S. Perazzini^{14,d}, E. Perez Trigo³⁷, P. Perret⁵, M. Perrin-Terrin⁶,
 L. Pescatore⁴⁵, E. Pesen⁶⁶, K. Petridis⁵³, A. Petrolini^{19,j}, E. Picatoste Olloqui³⁶, B. Pietrzyk⁴,
 T. Pilar⁴⁸, D. Pinci²⁵, A. Pistone¹⁹, S. Playfer⁵⁰, M. Plo Casasus³⁷, F. Polci⁸, A. Poluektov^{48,34},
 E. Polcarpo², A. Popov³⁵, D. Popov¹⁰, B. Popovici²⁹, C. Potterat², A. Powell⁵⁵,
 J. Prisciandaro³⁹, A. Pritchard⁵², C. Prouve⁴⁶, V. Pugatch⁴⁴, A. Puig Navarro³⁹, G. Punzi^{23,r},
 W. Qian⁴, B. Rachwal²⁶, J.H. Rademacker⁴⁶, B. Rakotomiaramanana³⁹, M. Rama¹⁸,
 M.S. Rangel², I. Raniuk⁴³, N. Rauschmayr³⁸, G. Raven⁴², S. Reichert⁵⁴, M.M. Reid⁴⁸,
 A.C. dos Reis¹, S. Ricciardi⁴⁹, A. Richards⁵³, M. Rihl³⁸, K. Rinnert⁵², V. Rives Molina³⁶,
 D.A. Roa Romero⁵, P. Robbe⁷, A.B. Rodrigues¹, E. Rodrigues⁵⁴, P. Rodriguez Perez⁵⁴,
 S. Roiser³⁸, V. Romanovsky³⁵, A. Romero Vidal³⁷, M. Rotondo²², J. Rouvinet³⁹, T. Ruf³⁸,
 F. Ruffini²³, H. Ruiz³⁶, P. Ruiz Valls⁶⁴, G. Sabatino^{25,l}, J.J. Saborido Silva³⁷, N. Sagidova³⁰,
 P. Sail⁵¹, B. Saitta^{15,e}, V. Salustino Guimaraes², C. Sanchez Mayordomo⁶⁴,
 B. Sanmartin Sedes³⁷, R. Santacesaria²⁵, C. Santamarina Rios³⁷, E. Santovetti^{24,l}, M. Sapunov⁶,
 A. Sarti^{18,m}, C. Satriano^{25,n}, A. Satta²⁴, M. Savrie^{16,f}, D. Savrina^{31,32}, M. Schiller⁴²,

H. Schindler³⁸, M. Schlupp⁹, M. Schmelling¹⁰, B. Schmidt³⁸, O. Schneider³⁹, A. Schopper³⁸, M.-H. Schune⁷, R. Schwemmer³⁸, B. Sciascia¹⁸, A. Sciubba²⁵, M. Seco³⁷, A. Semennikov³¹, K. Senderowska²⁷, I. Sepp⁵³, N. Serra⁴⁰, J. Serrano⁶, L. Sestini²², P. Seyfert¹¹, M. Shapkin³⁵, I. Shapoval^{16,43,f}, Y. Shcheglov³⁰, T. Shears⁵², L. Shekhtman³⁴, V. Shevchenko⁶³, A. Shires⁹, R. Silva Coutinho⁴⁸, G. Simi²², M. Sirendi⁴⁷, N. Skidmore⁴⁶, T. Skwarnicki⁵⁹, N.A. Smith⁵², E. Smith^{55,49}, E. Smith⁵³, J. Smith⁴⁷, M. Smith⁵⁴, H. Snoek⁴¹, M.D. Sokoloff⁵⁷, F.J.P. Soler⁵¹, F. Soomro³⁹, D. Souza⁴⁶, B. Souza De Paula², B. Spaan⁹, A. Sparkes⁵⁰, F. Spinella²³, P. Spradlin⁵¹, F. Stagni³⁸, S. Stahl¹¹, O. Steinkamp⁴⁰, O. Stenyakin³⁵, S. Stevenson⁵⁵, S. Stoica²⁹, S. Stone⁵⁹, B. Storaci⁴⁰, S. Stracka^{23,38}, M. Straticiu²⁹, U. Straumann⁴⁰, R. Stroili²², V.K. Subbiah³⁸, L. Sun⁵⁷, W. Sutcliffe⁵³, K. Swientek²⁷, S. Swientek⁹, V. Syropoulos⁴², M. Szczekowski²⁸, P. Szczypka^{39,38}, D. Szilard², T. Szumlak²⁷, S. T’Jampens⁴, M. Teklishyn⁷, G. Tellarini^{16,f}, F. Teubert³⁸, C. Thomas⁵⁵, E. Thomas³⁸, J. van Tilburg⁴¹, V. Tisserand⁴, M. Tobin³⁹, S. Tol⁴², L. Tomassetti^{16,f}, D. Tonelli³⁸, S. Topp-Joergensen⁵⁵, N. Torr⁵⁵, E. Tournefier⁴, S. Tourneur³⁹, M.T. Tran³⁹, M. Tresch⁴⁰, A. Tsaregorodtsev⁶, P. Tsopelas⁴¹, N. Tuning⁴¹, M. Ubeda Garcia³⁸, A. Ukleja²⁸, A. Ustyuzhanin⁶³, U. Uwer¹¹, V. Vagnoni¹⁴, G. Valenti¹⁴, A. Vallier⁷, R. Vazquez Gomez¹⁸, P. Vazquez Regueiro³⁷, C. Vázquez Sierra³⁷, S. Vecchi¹⁶, J.J. Velthuis⁴⁶, M. Veltri^{17,h}, G. Veneziano³⁹, M. Vesterinen¹¹, B. Viaud⁷, D. Vieira², M. Vieites Diaz³⁷, X. Vilasis-Cardona^{36,o}, A. Vollhardt⁴⁰, D. Volyansky¹⁰, D. Voong⁴⁶, A. Vorobyev³⁰, V. Vorobyev³⁴, C. Vob⁶², H. Voss¹⁰, J.A. de Vries⁴¹, R. Waldi⁶², C. Wallace⁴⁸, R. Wallace¹², J. Walsh²³, S. Wandernoth¹¹, J. Wang⁵⁹, D.R. Ward⁴⁷, N.K. Watson⁴⁵, D. Websdale⁵³, M. Whitehead⁴⁸, J. Wicht³⁸, D. Wiedner¹¹, G. Wilkinson⁵⁵, M.P. Williams⁴⁵, M. Williams⁵⁶, F.F. Wilson⁴⁹, J. Wimberley⁵⁸, J. Wishahi⁹, W. Wislicki²⁸, M. Witek²⁶, G. Wormser⁷, S.A. Wotton⁴⁷, S. Wright⁴⁷, S. Wu³, K. Wyllie³⁸, Y. Xie⁶¹, Z. Xing⁵⁹, Z. Xu³⁹, Z. Yang³, X. Yuan³, O. Yushchenko³⁵, M. Zangoli¹⁴, M. Zavertyaev^{10,b}, F. Zhang³, L. Zhang⁵⁹, W.C. Zhang¹², Y. Zhang³, A. Zhelezov¹¹, A. Zhokhov³¹, L. Zhong³, A. Zvyagin³⁸.

¹ Centro Brasileiro de Pesquisas Físicas (CBPF), Rio de Janeiro, Brazil

² Universidade Federal do Rio de Janeiro (UFRJ), Rio de Janeiro, Brazil

³ Center for High Energy Physics, Tsinghua University, Beijing, China

⁴ LAPP, Université de Savoie, CNRS/IN2P3, Annecy-Le-Vieux, France

⁵ Clermont Université, Université Blaise Pascal, CNRS/IN2P3, LPC, Clermont-Ferrand, France

⁶ CPPM, Aix-Marseille Université, CNRS/IN2P3, Marseille, France

⁷ LAL, Université Paris-Sud, CNRS/IN2P3, Orsay, France

⁸ LPNHE, Université Pierre et Marie Curie, Université Paris Diderot, CNRS/IN2P3, Paris, France

⁹ Fakultät Physik, Technische Universität Dortmund, Dortmund, Germany

¹⁰ Max-Planck-Institut für Kernphysik (MPIK), Heidelberg, Germany

¹¹ Physikalisches Institut, Ruprecht-Karls-Universität Heidelberg, Heidelberg, Germany

¹² School of Physics, University College Dublin, Dublin, Ireland

¹³ Sezione INFN di Bari, Bari, Italy

¹⁴ Sezione INFN di Bologna, Bologna, Italy

¹⁵ Sezione INFN di Cagliari, Cagliari, Italy

¹⁶ Sezione INFN di Ferrara, Ferrara, Italy

¹⁷ Sezione INFN di Firenze, Firenze, Italy

¹⁸ Laboratori Nazionali dell’INFN di Frascati, Frascati, Italy

¹⁹ Sezione INFN di Genova, Genova, Italy

²⁰ Sezione INFN di Milano Bicocca, Milano, Italy

²¹ Sezione INFN di Milano, Milano, Italy

²² Sezione INFN di Padova, Padova, Italy

- ²³ *Sezione INFN di Pisa, Pisa, Italy*
- ²⁴ *Sezione INFN di Roma Tor Vergata, Roma, Italy*
- ²⁵ *Sezione INFN di Roma La Sapienza, Roma, Italy*
- ²⁶ *Henryk Niewodniczanski Institute of Nuclear Physics Polish Academy of Sciences, Kraków, Poland*
- ²⁷ *AGH - University of Science and Technology, Faculty of Physics and Applied Computer Science, Kraków, Poland*
- ²⁸ *National Center for Nuclear Research (NCBJ), Warsaw, Poland*
- ²⁹ *Horia Hulubei National Institute of Physics and Nuclear Engineering, Bucharest-Magurele, Romania*
- ³⁰ *Petersburg Nuclear Physics Institute (PNPI), Gatchina, Russia*
- ³¹ *Institute of Theoretical and Experimental Physics (ITEP), Moscow, Russia*
- ³² *Institute of Nuclear Physics, Moscow State University (SINP MSU), Moscow, Russia*
- ³³ *Institute for Nuclear Research of the Russian Academy of Sciences (INR RAN), Moscow, Russia*
- ³⁴ *Budker Institute of Nuclear Physics (SB RAS) and Novosibirsk State University, Novosibirsk, Russia*
- ³⁵ *Institute for High Energy Physics (IHEP), Protvino, Russia*
- ³⁶ *Universitat de Barcelona, Barcelona, Spain*
- ³⁷ *Universidad de Santiago de Compostela, Santiago de Compostela, Spain*
- ³⁸ *European Organization for Nuclear Research (CERN), Geneva, Switzerland*
- ³⁹ *Ecole Polytechnique Fédérale de Lausanne (EPFL), Lausanne, Switzerland*
- ⁴⁰ *Physik-Institut, Universität Zürich, Zürich, Switzerland*
- ⁴¹ *Nikhef National Institute for Subatomic Physics, Amsterdam, The Netherlands*
- ⁴² *Nikhef National Institute for Subatomic Physics and VU University Amsterdam, Amsterdam, The Netherlands*
- ⁴³ *NSC Kharkiv Institute of Physics and Technology (NSC KIPT), Kharkiv, Ukraine*
- ⁴⁴ *Institute for Nuclear Research of the National Academy of Sciences (KINR), Kyiv, Ukraine*
- ⁴⁵ *University of Birmingham, Birmingham, United Kingdom*
- ⁴⁶ *H.H. Wills Physics Laboratory, University of Bristol, Bristol, United Kingdom*
- ⁴⁷ *Cavendish Laboratory, University of Cambridge, Cambridge, United Kingdom*
- ⁴⁸ *Department of Physics, University of Warwick, Coventry, United Kingdom*
- ⁴⁹ *STFC Rutherford Appleton Laboratory, Didcot, United Kingdom*
- ⁵⁰ *School of Physics and Astronomy, University of Edinburgh, Edinburgh, United Kingdom*
- ⁵¹ *School of Physics and Astronomy, University of Glasgow, Glasgow, United Kingdom*
- ⁵² *Oliver Lodge Laboratory, University of Liverpool, Liverpool, United Kingdom*
- ⁵³ *Imperial College London, London, United Kingdom*
- ⁵⁴ *School of Physics and Astronomy, University of Manchester, Manchester, United Kingdom*
- ⁵⁵ *Department of Physics, University of Oxford, Oxford, United Kingdom*
- ⁵⁶ *Massachusetts Institute of Technology, Cambridge, MA, United States*
- ⁵⁷ *University of Cincinnati, Cincinnati, OH, United States*
- ⁵⁸ *University of Maryland, College Park, MD, United States*
- ⁵⁹ *Syracuse University, Syracuse, NY, United States*
- ⁶⁰ *Pontifícia Universidade Católica do Rio de Janeiro (PUC-Rio), Rio de Janeiro, Brazil, associated to ²*
- ⁶¹ *Institute of Particle Physics, Central China Normal University, Wuhan, Hubei, China, associated to ³*
- ⁶² *Institut für Physik, Universität Rostock, Rostock, Germany, associated to ¹¹*
- ⁶³ *National Research Centre Kurchatov Institute, Moscow, Russia, associated to ³¹*
- ⁶⁴ *Instituto de Fisica Corpuscular (IFIC), Universitat de Valencia-CSIC, Valencia, Spain, associated to ³⁶*
- ⁶⁵ *KVI - University of Groningen, Groningen, The Netherlands, associated to ⁴¹*
- ⁶⁶ *Celal Bayar University, Manisa, Turkey, associated to ³⁸*

^a *Universidade Federal do Triângulo Mineiro (UFTM), Uberaba-MG, Brazil*

^b *P.N. Lebedev Physical Institute, Russian Academy of Science (LPI RAS), Moscow, Russia*

^c *Università di Bari, Bari, Italy*

^d *Università di Bologna, Bologna, Italy*

^e *Università di Cagliari, Cagliari, Italy*

- ^f Università di Ferrara, Ferrara, Italy*
- ^g Università di Firenze, Firenze, Italy*
- ^h Università di Urbino, Urbino, Italy*
- ⁱ Università di Modena e Reggio Emilia, Modena, Italy*
- ^j Università di Genova, Genova, Italy*
- ^k Università di Milano Bicocca, Milano, Italy*
- ^l Università di Roma Tor Vergata, Roma, Italy*
- ^m Università di Roma La Sapienza, Roma, Italy*
- ⁿ Università della Basilicata, Potenza, Italy*
- ^o LIFAELS, La Salle, Universitat Ramon Llull, Barcelona, Spain*
- ^p Hanoi University of Science, Hanoi, Viet Nam*
- ^q Università di Padova, Padova, Italy*
- ^r Università di Pisa, Pisa, Italy*
- ^s Scuola Normale Superiore, Pisa, Italy*
- ^t Università degli Studi di Milano, Milano, Italy*

1 Introduction

Heavy quarkonia are produced at the early stage of ultra-relativistic heavy-ion collisions and probe the existence of the quark-gluon plasma (QGP), a hot and dense nuclear medium. Due to colour screening effects in the QGP, the yield of heavy quarkonia in heavy-ion collisions is expected to be suppressed with respect to proton-proton (pp) collisions [1]. Heavy quarkonium production can also be suppressed by normal nuclear matter effects, often referred to as cold nuclear matter (CNM) effects, such as nuclear shadowing (antishadowing) effects, energy loss of the heavy quark or the heavy quark pair in the medium or nuclear absorption. Shadowing and antishadowing effects [2–6] describe how the parton densities are modified when a nucleon is bound inside a nucleus. A coherent treatment of energy loss for the initial state partons and final state $c\bar{c}$ or $b\bar{b}$ pairs in nuclear matter is described in Refs. [7, 8]. Nuclear absorption is a final-state effect caused by the break-up of these pairs due to the inelastic scattering with the nucleons. The importance of studying absorption effects for quarkonia in the high energy heavy-ion proton collisions is discussed in Refs. [9–11], and the energy and rapidity dependence was studied in Ref. [12]. The main models describing quarkonium production in hadron collisions are the colour-singlet model (CSM) [13–16], the colour-evaporation model (CEM) [17] and non-relativistic quantum chromodynamics (NRQCD) [18–21].

The pA collisions in which a QGP is not expected to be created, provide a unique opportunity to study CNM effects and to constrain the nuclear parton distribution functions describing the partonic structure of matter. These measurements offer crucial information to disentangle CNM effects from the effects of QGP in nucleus-nucleus collisions. Several measurements of CNM effects were performed by the fixed-target experiments at the SPS [22–25], Fermilab [26] and DESY [27]. With the proton-lead (pPb) data collected in 2013, CNM effects have been studied by the LHCb experiment with measurements of the differential production cross-sections of prompt J/ψ mesons and J/ψ from b -hadron decays [28], and by the ALICE experiment using measurements of inclusive J/ψ production [29]. Unambiguous CNM effects have been observed, in agreement with theoretical predictions.

The study of bottomonia, $\Upsilon(1S)$, $\Upsilon(2S)$ and $\Upsilon(3S)$ mesons, denoted generically by Υ in the following, provides complementary information about CNM effects to that from J/ψ production. For example, the $\Upsilon(1S)$ meson can survive in the QGP at higher temperatures than other heavy quarkonia owing to its higher binding energy [30, 31]. As a consequence, based on the prediction that the dissociation of Υ states in the QGP occurs sequentially according to their different binding energies [31], it is interesting to determine the production ratios of excited Υ mesons,

$$R^{nS/1S} \equiv \frac{\sigma(\Upsilon(nS)) \times \mathcal{B}(\Upsilon(nS) \rightarrow \mu^+ \mu^-)}{\sigma(\Upsilon(1S)) \times \mathcal{B}(\Upsilon(1S) \rightarrow \mu^+ \mu^-)}, \quad n = 2, 3, \quad (1)$$

where σ represents the cross-section for the production of the indicated meson and \mathcal{B} represents the branching fraction for its dimuon decay mode. The production ratios $R^{nS/1S}$ have been measured in pPb [32] and $PbPb$ [33] collisions for central rapidities by the CMS

experiment and the ratios of these quantities to $R^{nS/1S}$ measured in pp collisions show clear sequential suppression of Υ production, which indicates stronger (cold or hot) nuclear matter effects on the excited Υ states. LHCb can extend those studies to the forward and backward rapidity regions. From the theoretical point of view, predictions for bottomonia are more reliable than those for charmonia owing to the heavier quark masses and lower quark velocities.

In this analysis, the inclusive production cross-sections of Υ mesons are measured in $p\text{Pb}$ collisions at a nucleon-nucleon centre-of-mass energy $\sqrt{s_{NN}} = 5 \text{ TeV}$ at LHCb. Based on the cross-section measurements, the production ratios $R^{nS/1S}$ are evaluated and the CNM effects for $\Upsilon(1S)$ mesons are studied. The LHCb detector is a single-arm forward spectrometer [34] that covers the pseudorapidity region $2 < \eta < 5$ in pp collisions. To allow for measurements of pA collisions at both positive and negative rapidity, where rapidity is defined with respect to the direction of the proton, the proton and lead beams were interchanged approximately halfway during the $p\text{Pb}$ data taking period. Owing to the asymmetry in the energy per nucleon in the two beams, the nucleon-nucleon centre-of-mass system has a rapidity of $+0.465$ (-0.465) in the laboratory frame for the forward (backward) collisions, where forward (backward) is defined as positive (negative) rapidity. For the measurements described here rapidity ranges of $1.5 < y < 4.0$ and $-5.0 < y < -2.5$ are studied.

2 Detector and data set

The LHCb detector [34] is designed for the study of particles containing b or c quarks. The detector includes a high-precision tracking system consisting of a silicon-strip vertex detector (VELO) surrounding the interaction region, a large-area silicon-strip detector located upstream of a dipole magnet with a bending power of about 4 Tm , and three stations of silicon-strip detectors and straw drift tubes [35] placed downstream of the magnet. The combined tracking system provides a momentum resolution with a relative uncertainty that varies from 0.4% at low momentum to 0.6% at $100 \text{ GeV}/c$, and an impact parameter measurement with a resolution of $20 \mu\text{m}$ for charged particles with large transverse momentum, p_T . Different types of charged hadrons are distinguished using information from two ring-imaging Cherenkov (RICH) detectors [36]. Photon, electron and hadron candidates are identified by a calorimeter system consisting of scintillating-pad and preshower detectors, an electromagnetic calorimeter and a hadronic calorimeter. Muons are identified by a system composed of alternating layers of iron and multiwire proportional chambers [37]. The trigger [38] consists of a hardware stage, based on information from the calorimeter and muon systems, followed by a software stage, which applies a full event reconstruction.

The data sample used for this analysis was acquired during the $p\text{Pb}$ run in early 2013 and corresponds to an integrated luminosity of 1.1 nb^{-1} (0.5 nb^{-1}) for forward (backward) collisions. The hardware trigger was employed as an interaction trigger that rejected empty events. The software trigger required one well-reconstructed charged particle with hits in

the muon system and a transverse momentum greater than 600 MeV/ c .

Simulated samples based on pp collisions at 8 TeV are reweighted according to the track multiplicity to reproduce the experimental data at 5 TeV. The effect of the asymmetric beam energies in $p\text{Pb}$ collisions and different detector occupancies have been taken into account for the determination of the efficiencies. In the simulation, pp collisions are generated using PYTHIA 6.4 [39] with a specific LHCb configuration [40]. Hadron decays are described by EVTGEN [41], where final-state radiation is generated using PHOTOS [42]. The interactions of the generated particles with the detector and its response are implemented using the GEANT4 toolkit [43] as described in Ref. [44].

3 Cross-section determination

The total cross-section is measured for $\Upsilon(1S)$, $\Upsilon(2S)$ and $\Upsilon(3S)$ mesons in the kinematic region $p_{\text{T}} < 15$ GeV/ c and $1.5 < y < 4.0$ ($-5.0 < y < -2.5$) for the forward (backward) sample. The cross-section is also measured in the common rapidity coverage of the forward and backward samples, $2.5 < |y| < 4.0$, to study CNM effects. The product of the total production cross-sections and the branching fractions for $\Upsilon(nS)$ mesons is given by

$$\sigma(\Upsilon(nS)) \times \mathcal{B}(\Upsilon(nS) \rightarrow \mu^+\mu^-) = \frac{N^{\text{cor}}(\Upsilon(nS) \rightarrow \mu^+\mu^-)}{\mathcal{L}}, \quad n = 1, 2, 3, \quad (2)$$

where $N^{\text{cor}}(\Upsilon(nS) \rightarrow \mu^+\mu^-)$ is the efficiency-corrected number of signal candidates reconstructed with dimuon final states in the given p_{T} and y region, and \mathcal{L} is the integrated luminosity, calibrated by means of van der Meer scans [28, 45] for each beam configuration separately.

The strategy for the Υ cross-section measurement follows Refs. [46–48]. The Υ candidates are reconstructed from two oppositely charged particles consistent with a muon hypothesis based on particle identification information from the RICH detectors, the calorimeters and the muon system. Each particle must have a p_{T} above 1 GeV/ c and a good track fit quality. The two muon candidates are required to originate from a common vertex.

An unbinned extended maximum likelihood fit to the invariant mass distribution of the selected candidates is performed to determine the signal yields of $\Upsilon(1S)$, $\Upsilon(2S)$ and $\Upsilon(3S)$ mesons in a fit range $8400 < m_{\mu^+\mu^-} < 11400$ MeV/ c^2 . To describe the $\Upsilon(1S)$, $\Upsilon(2S)$ and $\Upsilon(3S)$ signal components, a sum of three Crystal Ball (CB) functions [49] is used, while the combinatorial background is modelled with an exponential function.

The shape parameters of the CB functions have been fixed using large samples collected in pp collisions [47], which determine the mass resolution for the $\Upsilon(1S)$ to be 43.0 MeV/ c^2 . The resolutions for the $\Upsilon(2S)$ and $\Upsilon(3S)$ signals are obtained by scaling this value by the ratio of their masses to the $\Upsilon(1S)$ meson mass [50].

Figure 1 shows the dimuon invariant mass distributions in the $p\text{Pb}$ forward and backward samples, with the fit results superimposed. In the backward sample higher combinatorial background is observed due to the larger track multiplicity. The signal

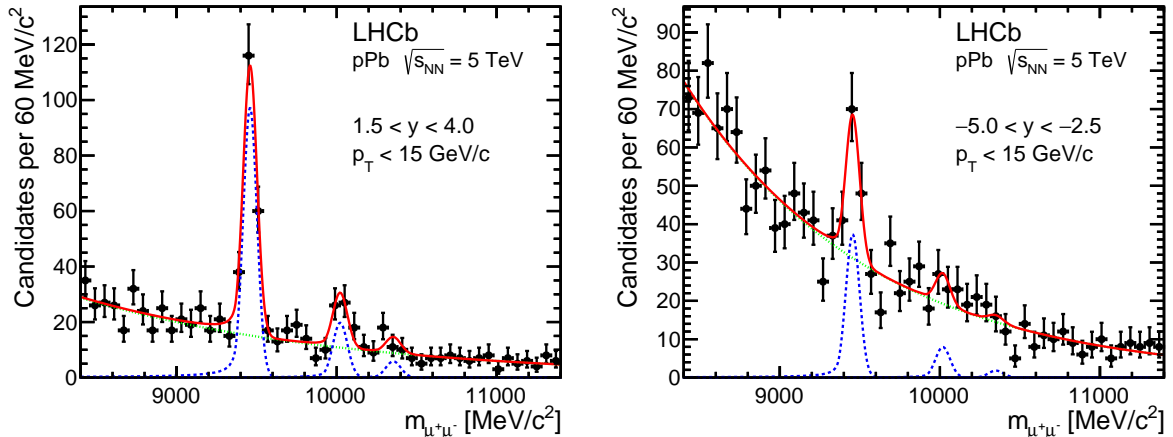


Figure 1: Invariant mass distribution of $\mu^+\mu^-$ pairs in the (left) forward and (right) backward samples of $p\text{Pb}$ collisions. The transverse momentum range is $p_T < 15 \text{ GeV}/c$. The rapidity range is $1.5 < y < 4.0$ ($-5.0 < y < -2.5$) for the forward (backward) sample. The black dots are the data points, the blue dashed curve indicates the signal component, the green dotted curve represents the combinatorial background, and the red solid curve is the sum of the signal and background components.

yields obtained from the fit are $N_{\Upsilon(1S)} = 189 \pm 16$ (72 ± 14), $N_{\Upsilon(2S)} = 41 \pm 9$ (17 ± 10), and $N_{\Upsilon(3S)} = 13 \pm 7$ (4 ± 8) in the forward (backward) sample. The yields of $\Upsilon(1S)$ mesons with $2.5 < |y| < 4.0$ are 122 ± 13 in the forward sample and 70 ± 13 in the backward sample. The uncertainties are statistical only.

A signal weight factor, ω_i , is assigned to each candidate using the *sPlot* technique [51] with the dimuon invariant mass as the discriminating variable. The efficiency-corrected signal yield N^{cor} is then calculated through an event-by-event efficiency correction ϵ_i as

$$N^{\text{cor}} = \sum_i \omega_i / \epsilon_i, \quad (3)$$

where the sum runs over all events. The total signal efficiency, which depends on the p_T and y of the Υ mesons, is the product of the geometric acceptance, reconstruction and selection, muon identification, and trigger efficiencies. The product of the acceptance, reconstruction and selection efficiencies is determined in fine p_T and y bins with simulated samples. The simulated events are reweighted according to the track multiplicity observed in data and corrected to account for small differences in the track-reconstruction efficiency between data and simulation [52, 53]. In the selected rapidity range the reconstruction and selection efficiency varies between 30% and 81%. The muon identification efficiency is obtained as a function of momentum and transverse momentum by a data-driven tag-and-probe approach using a $J/\psi \rightarrow \mu^+\mu^-$ sample [52]. For Υ candidates this efficiency is generally larger than 90%. The trigger efficiency was determined using a sample of $\Upsilon(1S)$ decays into muon pairs that did not require the muons to be in the trigger, and is around 95%. The corresponding uncertainty is described in the following section. Here

Table 1: Relative systematic uncertainties on the cross-sections, in percent, in the full rapidity range. The values in parenthesis refer specifically to $\Upsilon(1S)$ measurements when systematic uncertainties in the common rapidity range $2.5 < |y| < 4.0$ are notably different.

| Source | Forward | | | Backward | | |
|--------------------------|----------------|----------------|----------------|----------------|----------------|----------------|
| | $\Upsilon(1S)$ | $\Upsilon(2S)$ | $\Upsilon(3S)$ | $\Upsilon(1S)$ | $\Upsilon(2S)$ | $\Upsilon(3S)$ |
| Muon identification | 1.3 | 1.3 | 1.3 | 1.3 | 1.3 | 1.3 |
| Tracking efficiency | 1.5 | 1.5 | 1.5 | 1.5 | 1.5 | 1.5 |
| Mass fit model | 1.1 (1.0) | 4.9 | 13 | 1.8 (1.7) | 19 | 90 |
| Luminosity | 1.9 | 1.9 | 1.9 | 2.1 | 2.1 | 2.1 |
| Trigger | 2.1 | 2.1 | 2.1 | 5.0 | 5.0 | 5.0 |
| MC generation kinematics | 3.9 (3.8) | 3.9 | 3.9 | 7.6 (6.3) | 7.6 | 7.6 |
| Reconstruction | 1.5 | 1.5 | 1.5 | 1.5 | 1.5 | 1.5 |
| Total | 5.5 (5.4) | 7.3 | 14 | 9.8 (8.8) | 21 | 91 |

the much more abundant J/ψ decays are not used since the trigger efficiency depends on the muon transverse momentum.

4 Systematic uncertainties

The systematic uncertainties of this analysis are summarised in Table 1. They are added in quadrature to obtain the total systematic uncertainty.

Due to the finite size of the J/ψ calibration sample, the systematic uncertainty of the muon identification efficiency obtained from the tag-and-probe approach is 1.3%. The uncertainty due to the track reconstruction efficiency is estimated to be 1.5% by varying within its uncertainty the correction applied to the muon reconstruction efficiency.

The systematic uncertainty due to the choice of the fit model used to describe the shape of the dimuon mass distribution is estimated by varying the fixed parameters of the CB function, or by using a polynomial function, whose parameters are determined by the fit, to describe the background shape. The largest difference in yields of each resonance with respect to the nominal result is considered as the systematic uncertainty.

The luminosity is determined with an uncertainty of 1.9% (2.1%) for the p Pb forward (backward) sample from the rate of interactions that yield at least one reconstructed track in the VELO. The absolute calibration is determined with van der Meer scans, as described in Ref. [28].

The trigger efficiency in the forward sample is determined directly from the data using a sample unbiased by the trigger decision. The corresponding uncertainty is 2.1%. Due to the limited sample size, the trigger efficiency in the backward sample is estimated using the forward sample, since it has been observed that the dependence of trigger efficiencies on the charged-particle multiplicity is small [28]. The systematic uncertainty is 5.0%, taking

into account the difference between the trigger efficiencies obtained using the forward and backward samples.

An uncertainty is introduced by the possible difference between the data and simulation samples of the p_T and y spectra inside each bin. This is estimated by doubling the number of p_T or y bins in the efficiency tables based on the simulated samples. In the forward (backward) sample, the difference to the nominal binning is 3.9% (7.6%) in the full rapidity range, and 3.8% (6.3%) in the common rapidity coverage. These differences are taken as systematic uncertainties.

The systematic uncertainties due to reconstruction effects, *e.g.* track and vertexing quality, have been studied in the J/ψ analysis in p Pb collisions [28] and determined to be 1.5%.

Although the initial polarisation of the vector meson affects the efficiency, recent results show that the polarisations of the $\Upsilon(1S)$, $\Upsilon(2S)$ and $\Upsilon(3S)$ mesons are small in pp collisions [54]. In this analysis, we take them to be zero and do not assign any systematic uncertainty to account for this assumption.

5 Results

The products of production cross-sections and branching fractions for Υ mesons with $p_T < 15$ GeV/ c are measured for the different rapidity ranges to be

$$\begin{aligned}\sigma(\Upsilon(1S), -5.0 < y < -2.5) \times \mathcal{B}(1S) &= 295 \pm 56 \pm 29 \text{ nb}, \\ \sigma(\Upsilon(2S), -5.0 < y < -2.5) \times \mathcal{B}(2S) &= 81 \pm 39 \pm 18 \text{ nb}, \\ \sigma(\Upsilon(3S), -5.0 < y < -2.5) \times \mathcal{B}(3S) &= 5 \pm 26 \pm 5 \text{ nb}, \\ \sigma(\Upsilon(1S), 1.5 < y < 4.0) \times \mathcal{B}(1S) &= 380 \pm 35 \pm 21 \text{ nb}, \\ \sigma(\Upsilon(2S), 1.5 < y < 4.0) \times \mathcal{B}(2S) &= 75 \pm 19 \pm 5 \text{ nb}, \\ \sigma(\Upsilon(3S), 1.5 < y < 4.0) \times \mathcal{B}(3S) &= 27 \pm 16 \pm 4 \text{ nb},\end{aligned}$$

where the first uncertainty is statistical and the second systematic, a convention also used in the following. The variation in relative size of the statistical uncertainty compared to the signal yields is due to the variation of the event-by-event efficiencies and the variation of the signal-to-background ratio over the accessible phase space. In the common rapidity range $2.5 < |y| < 4.0$, the results for $\Upsilon(1S)$ production are

$$\begin{aligned}\sigma(\Upsilon(1S), -4.0 < y < -2.5) \times \mathcal{B}(1S) &= 282 \pm 53 \pm 25 \text{ nb}, \\ \sigma(\Upsilon(1S), 2.5 < y < 4.0) \times \mathcal{B}(1S) &= 211 \pm 23 \pm 11 \text{ nb}.\end{aligned}$$

Using the results described above, the production ratios $R^{nS/1S}$ are measured to be

$$\begin{aligned}R^{2S/1S}(-5.0 < y < -2.5) &= 0.28 \pm 0.14 \pm 0.05, \\ R^{3S/1S}(-5.0 < y < -2.5) &= 0.02 \pm 0.09 \pm 0.02, \\ R^{2S/1S}(1.5 < y < 4.0) &= 0.20 \pm 0.05 \pm 0.01, \\ R^{3S/1S}(1.5 < y < 4.0) &= 0.07 \pm 0.04 \pm 0.01.\end{aligned}$$

In these ratios all the systematic uncertainties cancel except for those due to the mass fit model. The measurements of $R^{nS/1S}$ in $p\text{Pb}$ collisions are compatible with those in pp collisions [46–48].

The nuclear modification factor $R_{p\text{Pb}}(\sqrt{s_{NN}}) \equiv \sigma_{p\text{Pb}}(\sqrt{s_{NN}})/(A \times \sigma_{pp}(\sqrt{s_{NN}}))$ is used to study the CNM effects, where A is the atomic mass number of the nucleus and $\sqrt{s_{NN}}$ is the centre-of-mass energy of the nucleon-nucleon system. The determination of $R_{p\text{Pb}}$ requires the value of the production cross-section in pp collisions at 5 TeV, for which no data is yet available. Following the same approach as in the measurement of $R_{p\text{Pb}}$ for J/ψ mesons [28], this cross-section is obtained by a power-law interpolation from previous LHCb measurements [46–48] in the range $p_T < 15 \text{ GeV}/c$ and $2.5 < y < 4.0$ [55]. The product of the production cross-section and the dimuon branching fraction for $\Upsilon(1S)$ mesons in pp collisions at 5 TeV, with $p_T < 15 \text{ GeV}/c$ and $2.5 < y < 4.0$, is $\sigma_{pp} \times \mathcal{B}(1S) = 1.12 \pm 0.11 \text{ nb}$, from which the nuclear modification factors $R_{p\text{Pb}}$ for $\Upsilon(1S)$ mesons in the ranges $-4.0 < y < -2.5$ and $2.5 < y < 4.0$ are determined to be

$$\begin{aligned} R_{p\text{Pb}}(\Upsilon(1S), -4.0 < y < -2.5) &= 1.21 \pm 0.23 \pm 0.12, \\ R_{p\text{Pb}}(\Upsilon(1S), 2.5 < y < 4.0) &= 0.90 \pm 0.10 \pm 0.09. \end{aligned}$$

Figure 2 shows the measurement of $R_{p\text{Pb}}$ for $\Upsilon(1S)$ mesons as a function of rapidity. Relative to the $\Upsilon(1S)$ production in pp collisions, the data are consistent with a suppression in the forward region and an enhancement due to antishadowing effects in the backward hemisphere. In the forward region, the data suggest that the suppression of $\Upsilon(1S)$ production is smaller than that of prompt J/ψ production. The central value of $R_{p\text{Pb}}$ for $\Upsilon(1S)$ mesons is close to that for J/ψ from b -hadron decays, which reflects the CNM effects on b hadrons. Within the sizable uncertainties of the current measurements, the result agrees with existing theoretical predictions [3, 6, 7]. The calculations in Ref. [6] are based on the leading-order CSM, taking into account the modification of the gluon distribution functions in the nucleus with the parameterisation EPS09 [56]. The predictions in Ref. [3] use the next-to-leading-order CEM and the parton shadowing is calculated with the EPS09 parameterisation. Theoretical predictions of the coherent energy loss effect are provided in Ref. [7], both with and without additional parton shadowing effects as parameterised with EPS09.

Another observable that characterises CNM effects is the forward-backward production ratio, defined as $R_{\text{FB}}(\sqrt{s_{NN}}, |y|) \equiv \sigma(\sqrt{s_{NN}}, +|y|)/\sigma(\sqrt{s_{NN}}, -|y|)$. The ratio does not depend on the reference pp cross-section, and part of the experimental and theoretical uncertainties cancel. The forward-backward production ratio of $\Upsilon(1S)$ mesons is

$$R_{\text{FB}}(2.5 < |y| < 4.0) = 0.75 \pm 0.16 \pm 0.08.$$

Figure 3 shows the measured value of R_{FB} for $\Upsilon(1S)$ mesons as a function of absolute rapidity, together with the theoretical predictions [3, 6, 7] and R_{FB} , measured by LHCb, for prompt J/ψ mesons and J/ψ from b hadrons [28]. Measurements and theoretical predictions agree.

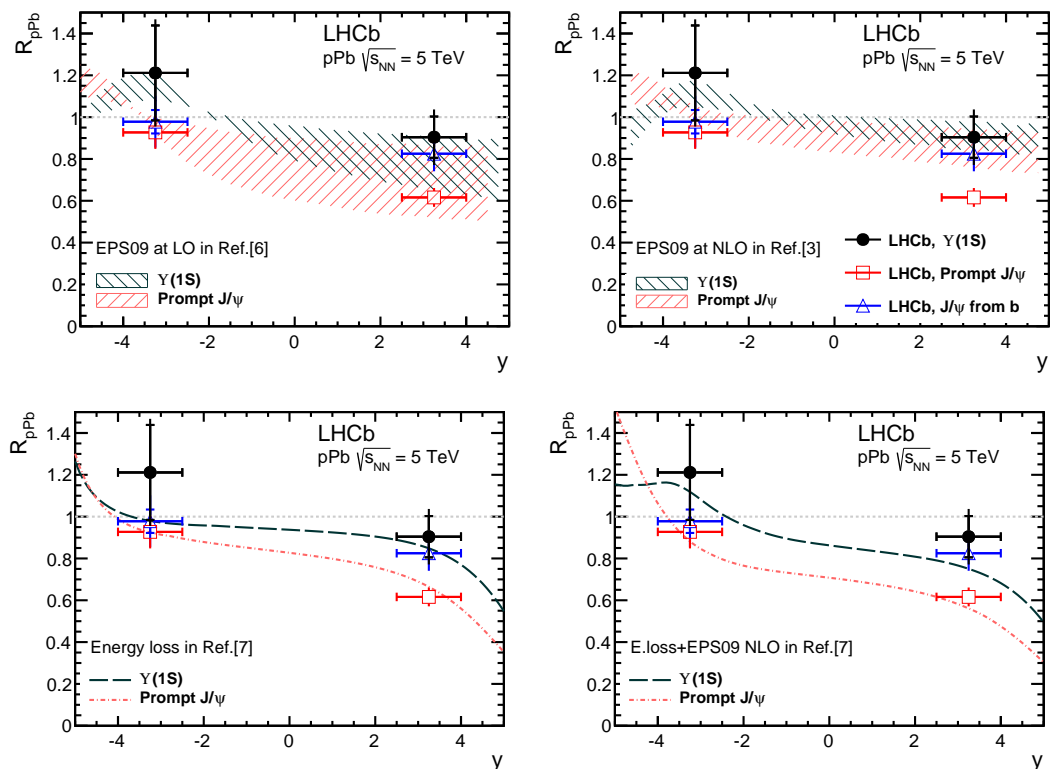


Figure 2: Nuclear modification factor, R_{pPb} , compared to other measurements and theoretical predictions. The black dots, red squares, and blue triangles indicate the LHCb measurements for $\Upsilon(1S)$ mesons, prompt J/ψ mesons, and J/ψ from b -hadron decays, respectively [28]. The inner error bars (delimited by the horizontal lines) show the statistical uncertainties; the outer ones show the statistical and systematic uncertainties added in quadrature. The data are compared with theoretical predictions for Υ and prompt J/ψ mesons from different models, one per panel. The shaded areas indicate the uncertainties of the theoretical calculations.

6 Conclusions

The production of Υ mesons is studied in pPb collisions with the LHCb detector at a nucleon-nucleon centre-of-mass energy $\sqrt{s_{NN}} = 5$ TeV in the transverse momentum range of $p_T < 15$ GeV/ c and rapidity range $-5.0 < y < -2.5$ and $1.5 < y < 4.0$.

The nuclear modification factor for the $\Upsilon(1S)$ meson is determined using the cross-section of $\Upsilon(1S)$ production in pp collisions at 5 TeV interpolated from previous LHCb measurements. It is compatible with predictions of a suppression of $\Upsilon(1S)$ production with respect to pp collisions in the forward region and antishadowing effects in the backward region. The forward-backward production ratio of the $\Upsilon(1S)$ is also measured, and the result is consistent with existing theoretical predictions, where the nuclear shadowing effects are taken into account with the EPS09 parameterisation, or a coherent energy loss is considered. A first measurement of the production ratios of excited Υ mesons relative to the ground state Υ has been performed. Due to the small integrated luminosity of the available

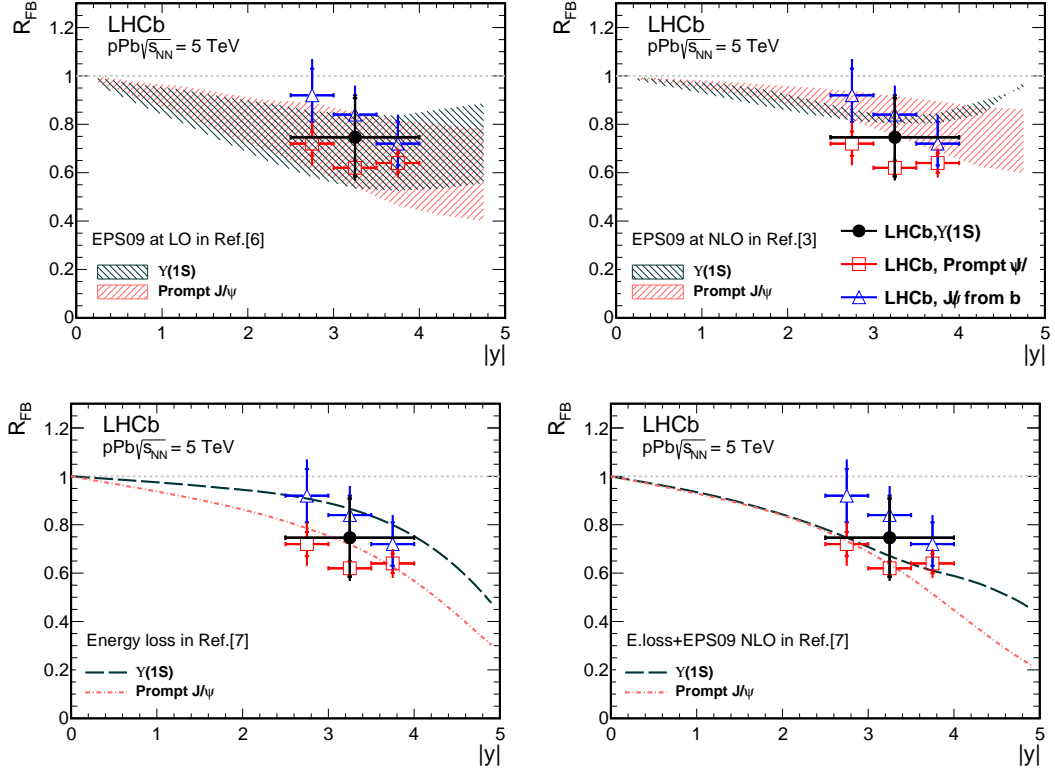


Figure 3: Forward-backward production ratio, R_{FB} , as a function of absolute rapidity. The black dots, red squares, and blue triangles indicate the LHCb measurements for $\Upsilon(1S)$ mesons, prompt J/ψ mesons, and J/ψ from b -hadron decays, respectively [28]. The inner error bars (delimited by the horizontal lines) show the statistical uncertainties; the outer ones show the statistical and systematic uncertainties added in quadrature. The data are compared with theoretical predictions for Υ and prompt J/ψ mesons from different models, one per panel. The shaded areas indicate the uncertainties of the theoretical calculations.

data sample, the measurements presented here, though very promising, have relatively large uncertainties. More pPb data would allow a precise quantitative investigation of cold nuclear matter effects, to establish a reliable baseline for the interpretations of related quark-gluon plasma signatures in nucleus-nucleus collisions and constrain the parameterizations of theoretical models.

Acknowledgements

We thank F. Arleo, J. P. Lansberg and R. Vogt for providing us with the theoretical predictions and for the stimulating and helpful discussions. We express our gratitude to our colleagues in the CERN accelerator departments for the excellent performance of the LHC. We thank the technical and administrative staff at the LHCb institutes. We acknowledge support from CERN and from the national agencies: CAPES, CNPq, FAPERJ and FINEP (Brazil); NSFC (China); CNRS/IN2P3 and Region Auvergne (France); BMBF, DFG, HGF and MPG (Germany); SFI (Ireland); INFN (Italy); FOM and NWO (The Netherlands); SCSR (Poland); MEN/IFA (Romania); MinES, Rosatom, RFBR and NRC “Kurchatov Institute” (Russia); MinECo, XuntaGal and GENCAT (Spain); SNSF and SER (Switzerland); NASU (Ukraine); STFC and the Royal Society (United Kingdom); NSF (USA). We also acknowledge the support received from EPLANET, Marie Curie Actions and the ERC under FP7. The Tier1 computing centres are supported by IN2P3 (France), KIT and BMBF (Germany), INFN (Italy), NWO and SURF (The Netherlands), PIC (Spain), GridPP (United Kingdom). We are indebted to the communities behind the multiple open source software packages on which we depend. We are also thankful for the computing resources and the access to software R&D tools provided by Yandex LLC (Russia).

References

- [1] T. Matsui and H. Satz, *J/ψ suppression by quark-gluon plasma formation*, Phys. Lett. **B178** (1986) 416.
- [2] E. G. Ferreira, F. Fleuret, J. P. Lansberg, and A. Rakotozafindrabe, *Impact of the nuclear modification of the gluon densities on J/ψ production in pPb collisions at $\sqrt{s_{NN}} = 5$ TeV*, Phys. Rev. **C88** (2013) 047901, [arXiv:1305.4569](#).
- [3] J. L. Albacete *et al.*, *Predictions for p+Pb collisions at $\sqrt{s_{NN}} = 5$ TeV*, Int. J. Mod. Phys. **E22** (2013) 1330007, [arXiv:1301.3395](#).
- [4] A. Adeluyi and T. Nguyen, *Coherent photoproduction of ψ and Υ mesons in ultraperipheral pPb and PbPb collisions at the CERN Large Hadron Collider at $\sqrt{s_{NN}} = 5$ TeV and $\sqrt{s_{NN}} = 2.76$ TeV*, Phys. Rev. **C87** (2013) 027901, [arXiv:1302.4288](#).
- [5] G. A. Chirilli, B.-W. Xiao, and F. Yuan, *Inclusive hadron productions in pA collisions*, Phys. Rev. **D86** (2012) 054005, [arXiv:1203.6139](#).
- [6] E. G. Ferreira *et al.*, *Υ production in p(d)A collisions at RHIC and the LHC*, Eur. Phys. J. **C73** (2011) 2427, [arXiv:1110.5047](#).
- [7] F. Arleo and S. Peigné, *Heavy-quarkonium suppression in p-A collisions from parton energy loss in cold QCD matter*, JHEP **03** (2013) 122, [arXiv:1212.0434](#).

- [8] F. Arleo, R. Kolevatov, S. Peigné, and M. Rustamova, *Centrality and p_{\perp} dependence of J/ψ suppression in proton-nucleus collisions from parton energy loss*, JHEP **05** (2013) 155, arXiv:1304.0901.
- [9] D. Kharzeev and H. Satz, *Charmonium composition and nuclear suppression*, Phys. Lett. **B366** (1996) 316, arXiv:hep-ph/9508276.
- [10] D. Kharzeev and H. Satz, *Charmonium interaction in nuclear matter*, Phys. Lett. **B356** (1995) 365, arXiv:hep-ph/9504397.
- [11] D. Kharzeev, C. Lourenço, M. Nardi, and H. Satz, *A Quantitative analysis of charmonium suppression in nuclear collisions*, Z. Phys. **C74** (1997) 307, arXiv:hep-ph/9612217.
- [12] C. Lourenco, R. Vogt, and H. K. Wöhri, *Energy dependence of J/ψ absorption in proton-nucleus collisions*, JHEP **02** (2009) 014, arXiv:0901.3054.
- [13] C.-H. Chang, *Hadronic production of J/ψ associated with a gluon*, Nucl. Phys. **B172** (1980) 425.
- [14] R. Baier and R. Ruckl, *Hadronic production of J/ψ and Υ : transverse momentum distributions*, Phys. Lett. **B102** (1981) 364.
- [15] J. Campbell, F. Maltoni, and F. Tramontano, *QCD corrections to J/ψ and Υ production at hadron colliders*, Phys. Rev. Lett. **98** (2007) 252002, arXiv:hep-ph/0703113.
- [16] P. Artoisenet *et al.*, *Υ production at Fermilab Tevatron and LHC energies*, Phys. Rev. Lett. **101** (2008) 152001, arXiv:0806.3282.
- [17] M. Glück, J. F. Owens, and E. Reya, *Gluon contribution to hadronic J/ψ production*, Phys. Rev. **D17** (1978) 2324.
- [18] G. T. Bodwin, E. Braaten, and G. P. Lepage, *Rigorous QCD analysis of inclusive annihilation and production of heavy quarkonium*, Phys. Rev. **D51** (1995) 1125, arXiv:hep-ph/9407339.
- [19] G. T. Bodwin, E. Braaten, and G. P. Lepage, *Erratum: Rigorous QCD analysis of inclusive annihilation and production of heavy quarkonium*, Phys. Rev. **D55** (1997) 5853.
- [20] P. L. Cho and A. K. Leibovich, *Color octet quarkonia production*, Phys. Rev. **D53** (1996) 150, arXiv:hep-ph/9505329.
- [21] P. L. Cho and A. K. Leibovich, *Color octet quarkonia production. 2.*, Phys. Rev. **D53** (1996) 6203, arXiv:hep-ph/9511315.
- [22] NA38 collaboration, M. Abreu *et al.*, *Charmonia production in 450 GeV/c proton induced reactions*, Phys. Lett. **B444** (1998) 516.

- [23] NA50 collaboration, B. Alessandro *et al.*, *J/ψ and ψ′ production and their normal nuclear absorption in proton-nucleus collisions at 400 GeV*, Eur. Phys. J. **C48** (2006) 329, arXiv:nucl-ex/0612012.
- [24] NA51 collaboration, M. Abreu *et al.*, *J/ψ, ψ′ and Drell-Yan production in pp and pd interactions at 450 GeV/c*, Phys. Lett. **B438** (1998) 35.
- [25] NA60 collaboration, R. Arnaldi *et al.*, *J/ψ production in proton-nucleus collisions at 158 and 400 GeV*, Phys. Lett. **B706** (2012) 263, arXiv:1004.5523.
- [26] FNAL E866/NuSea collaboration, M. J. Leitch *et al.*, *Measurement of differences between J/ψ and ψ′ suppression in p-A collisions*, Phys. Rev. Lett. **84** (2000) 3256, arXiv:nucl-ex/9909007.
- [27] HERA-B collaboration, I. Abt *et al.*, *Kinematic distributions and nuclear effects of J/ψ production in 920 GeV fixed-target proton-nucleus collisions*, Eur. Phys. J. **C60** (2009) 525, arXiv:0812.0734.
- [28] LHCb collaboration, R. Aaij *et al.*, *Study of J/ψ production and cold nuclear matter effects in pPb collisions at $\sqrt{s_{NN}} = 5$ TeV*, JHEP **02** (2014) 072, arXiv:1308.6729.
- [29] ALICE collaboration, B. B. Abelev *et al.*, *J/ψ production and nuclear effects in p-Pb collisions at $\sqrt{s_{NN}} = 5.02$ TeV*, JHEP **02** (2014) 073, arXiv:1308.6726.
- [30] F. Karsch and H. Satz, *The spectral analysis of strongly interacting matter*, Z. Phys. **C51** (1991) 209.
- [31] S. Digal, P. Petreczky, and H. Satz, *Quarkonium feed-down and sequential suppression*, Phys. Rev. **D64** (2001) 094015, arXiv:hep-ph/0106017.
- [32] CMS collaboration, S. Chatrchyan *et al.*, *Event activity dependence of $\Upsilon(nS)$ production in $\sqrt{s_{NN}} = 5.02$ TeV pPb and $\sqrt{s} = 2.76$ TeV pp collisions*, JHEP **04** (2014) 103, arXiv:1312.6300.
- [33] CMS collaboration, S. Chatrchyan *et al.*, *Observation of sequential Υ suppression in PbPb collisions*, Phys. Rev. Lett. **109** (2012) 222301, arXiv:1208.2826.
- [34] LHCb collaboration, A. A. Alves Jr. *et al.*, *The LHCb detector at the LHC*, JINST **3** (2008) S08005.
- [35] R. Arink *et al.*, *Performance of the LHCb Outer Tracker*, JINST **9** (2014) P01002, arXiv:1311.3893.
- [36] M. Adinolfi *et al.*, *Performance of the LHCb RICH detector at the LHC*, Eur. Phys. J. **C73** (2013) 2431, arXiv:1211.6759.
- [37] A. A. Alves Jr. *et al.*, *Performance of the LHCb muon system*, JINST **8** (2013) P02022, arXiv:1211.1346.

- [38] R. Aaij *et al.*, *The LHCb trigger and its performance in 2011*, JINST **8** (2013) P04022, [arXiv:1211.3055](#).
- [39] T. Sjöstrand, S. Mrenna, and P. Skands, *PYTHIA 6.4 physics and manual*, JHEP **05** (2006) 026, [arXiv:hep-ph/0603175](#).
- [40] I. Belyaev *et al.*, *Handling of the generation of primary events in GAUSS, the LHCb simulation framework*, Nuclear Science Symposium Conference Record (NSS/MIC) **IEEE** (2010) 1155.
- [41] D. J. Lange, *The EvtGen particle decay simulation package*, Nucl. Instrum. Meth. **A462** (2001) 152.
- [42] P. Golonka and Z. Was, *PHOTOS Monte Carlo: a precision tool for QED corrections in Z and W decays*, Eur. Phys. J. **C45** (2006) 97, [arXiv:hep-ph/0506026](#).
- [43] Geant4 collaboration, J. Allison *et al.*, *Geant4 developments and applications*, IEEE Trans. Nucl. Sci. **53** (2006) 270; Geant4 collaboration, S. Agostinelli *et al.*, *Geant4: a simulation toolkit*, Nucl. Instrum. Meth. **A506** (2003) 250.
- [44] M. Clemencic *et al.*, *The LHCb simulation application, GAUSS: design, evolution and experience*, J. Phys. Conf. Ser. **331** (2011) 032023.
- [45] S. van der Meer, *Calibration of the effective beam height in the ISR*, CERN report, CERN-ISR-PO-68-31 (1968).
- [46] LHCb collaboration, R. Aaij *et al.*, *Measurement of Υ production in pp collisions at $\sqrt{s} = 7$ TeV*, Eur. Phys. J. **C72** (2012) 2025, [arXiv:1202.6579](#).
- [47] LHCb collaboration, R. Aaij *et al.*, *Production of J/ψ and Υ mesons in pp collisions at $\sqrt{s} = 8$ TeV*, JHEP **06** (2013) 064, [arXiv:1304.6977](#).
- [48] LHCb collaboration, R. Aaij *et al.*, *Measurement of Υ production in pp collisions at $\sqrt{s} = 2.76$ TeV*, Eur. Phys. J. **C74** (2014) 2835, [arXiv:1402.2539](#).
- [49] T. Skwarnicki, *A study of the radiative cascade transitions between the Upsilon-prime and Upsilon resonances*, PhD thesis, Institute of Nuclear Physics, Krakow, 1986, DESY-F31-86-02.
- [50] Particle Data Group, J. Beringer *et al.*, *Review of particle physics*, Phys. Rev. **D86** (2012) 010001, and 2013 partial update for the 2014 edition.
- [51] M. Pivk and F. R. Le Diberder, *sPlot: a statistical tool to unfold data distributions*, Nucl. Instrum. Meth. **A555** (2005) 356, [arXiv:physics/0402083](#).
- [52] A. Jaeger *et al.*, *Measurement of the track finding efficiency*, CERN-LHCb-PUB-2011-025.

- [53] F. Archilli *et al.*, *Performance of the muon identification at LHCb*, JINST **8** (2013) P10020, [arXiv:1306.0249](#).
- [54] CMS collaboration, S. Chatrchyan *et al.*, *Measurement of the $\Upsilon(1S)$, $\Upsilon(2S)$, and $\Upsilon(3S)$ polarizations in pp collisions at $\sqrt{s} = 7$ TeV*, Phys. Rev. Lett. **110** (2013) 081802, [arXiv:1209.2922](#).
- [55] ALICE and LHCb collaborations, *Reference pp cross-sections for J/ψ studies in proton-lead collisions at $\sqrt{s_{NN}} = 5.02$ TeV and comparisons between ALICE and LHCb results*, LHCb-CONF-2013-013, ALICE-PUBLIC-2013-002 .
- [56] K. Eskola, H. Paukkunen, and C. Salgado, *EPS09 – a new generation of NLO and LO nuclear parton distribution functions*, JHEP **04** (2009) 065, [arXiv:0902.4154](#).